Modeling of seepage using a Eulerian-based finite element method

Jin Chen, Bipul Hawlader, Chen Wang
Memorial University of Newfoundland, St. John's, Canada
Kshama Roy
Northern Crescent Inc., Calgary, Canada
Kenton Pike
TechnipFMC, St. John's, Canada

ABSTRACT
Seepage plays a significant role in many geotechnical problems such as the stability of earth dams and riverbanks. In addition, the large-deformation behavior of soil is equally important in many cases, including progressive failure of slopes, and landslides in sensitive clays. The large-deformation can be successfully simulated using Eulerian-based finite-element (FE) modeling techniques. In the present study, a technique is developed for a Eulerian-based FE analysis using Abaqus FE software to simulate both transient and steady-state seepage through an earth dam. The FE simulation results, including the seepage, in-situ stresses and slip surface in slope stability analysis, are compared with the analyses using the GeoStudio software package. In terms of practical implication, the developed seepage model could be coupled with the large-deformation FE technique in Abaqus to simulate the progressive failure of a riverbank.

RÉSUMÉ
Les infiltrations jouent un rôle important dans de nombreux problèmes géotechniques tels que la stabilité des barrages en terre et des berges des rivières. De plus, le comportement du sol en grandes déformations est tout aussi important, y compris la rupture progressive des pentes et les glissements de terrain dans les argiles sensibles. Les grandes déformations peuvent être simulées avec succès à l'aide de techniques de modélisation par éléments finis (FE) basées sur Eulerian. Dans la présente étude, une technique est développée pour une analyse FE basée sur Eulerian utilisant le logiciel Abaqus FE pour simuler des infiltrations transitoires et stables à travers un barrage en terre. Les résultats de la simulation FE, y compris l'infiltration, les contraintes in situ et la surface de glissement dans l'analyse de la stabilité des pentes, sont comparés aux analyses effectuées à l'aide du logiciel GeoStudio. En termes d'implication pratique, le modèle de suintement développé pourrait être associé à la technique d'évaluation à grande déformation d'Abaqus pour simuler la défaillance progressive d'une rive.

1 INTRODUCTION

Seepage of water through soil could be a potential cause of slope failure. Seepage could alter both effective and total stresses in soil elements and thereby, the shear resistance. In addition, seepage force increases the driving force that could fail a slope which might be stable without seepage. For example, a high artesian groundwater condition along the Savail River in Quebec was recognized as one of the main causes of the 2010 St. Jude Landslide (Locat et al., 2011). The artesian groundwater condition and resulting seepage increased the pore water pressure, and thus reduced the effective stress and the shear strength of soils to nearly zero near the bottom of the river. This might have caused a small slide near the toe of the riverbank. Because of the stress redistribution, the failure then propagates further through the sensitive clays resulting in the large-scale St. Jude landslide on May 10, 2010. Note that seepage is not the only cause of a large-scale landslide. Many other factors are also involved in this process, e.g. in-situ stress condition, shear strength reduction, natural and human activities. In the present study, the role of seepage is primarily discussed.

Several methods have been developed in the past to conduct the slope stability analyses with seepage effects, e.g. limit equilibrium (LE), finite-element (FE). Among these methods, the LE method is widely used in the industry to assess the factor of safety (FOS) of the slope. By applying the precalculated seepage forces to the LE model, the FOS under steady-state seepage can be calculated. Locat et al. (2011) used the SLOPE/W software (GeoStudio, 2007), which is based on the LE theory, to conduct the slope stability analysis of the 2010 St. Jude Landslide. Prior to the LE analysis for stability, the groundwater condition was evaluated through a steady-state seepage modeling using SEEP/W software (GeoStudio, 2007). The LE analysis shows a similar first slip surface as observed in the field. However, the LE method failed to explain the formation of the horizontal shear plane, the horsts, and grabens.

The FE method has also been used for analyzing slope stability under seepage effects (Lane and Griffiths, 2000). The traditional Lagrangian-based FE method can capture the post-peak softening behavior of sensitive clay and strain localization in a slope stability analysis. However, a significant mesh distortion occurs during the large deformation and therefore, the traditional Lagrangian-based FE analysis cannot handle the large-deformation behavior of the slope failure, e.g., the progressive failure in a spread type of landslide.

The Eulerian-based FE approach has been used in the past for the large-deformation analysis of sensitive clay slope failures (Dey et al., 2015; 2016). The progressive failure of sensitive clay landslides was successfully modeled by using the Eulerian-based FE method. Comparison between FE and LE analysis of the failure of the first soil block for an undrained loading condition has been performed in Saha et al. (2014). However, in these studies, the effects of seepage were not considered. Hamann et al. (2015) showed that the partially drained condition (transient seepage), for pile jacking into a fully saturated soil, can be simulated in a Eulerian-based FE approach where the pore water pressure was simulated with the thermal–hydraulic analogy theory. However, the seepage condition in a slope has not been modeled to establish the in-situ stresses for a Eulerian-based FE code.

In the present study, a methodology based on the thermal–hydraulic analogy theory is proposed for the seepage modeling in a slope with a Eulerian-based FE code. The results are benchmarked with SEEP/W analysis. Furthermore, the in-situ stresses under the influence of the steady-state seepage are simulated by SIGMA/W and the Eulerian-based FE code, respectively. Finally, the strength reduction method is implemented to trigger the slope failure in the Eulerian-based FE code to compare with the LE results from SLOPE/W.

2 NUMERICAL MODELING TECHNIQUE

For numerical analyses, GeoStudio software package (SEEP/W, SIGMA/W, and SLOPE/W) and the Eulerian-based FE code available in Abaqus FE software are adopted for the seepage, in-situ stress and slope failure modeling.

2.1 GeoStudio

SEEP/W is a finite element software product, available in GeoStudio package, for modeling groundwater flow in porous media (soils). SEEP/W is capable of modeling both steady-state and transient seepage problems. Therefore, it has been widely applied in the analysis and design process of geotechnical engineering (Ng and Pang, 2000; Oh and Vanapalli, 2010).

SIGMA/W is also based on the finite element method. This software product can model stress and deformation in geotechnical problems with different constitutive models to represent a wide range of soils or structural materials (Oh and Vanapalli, 2011; Qi and Vanapalli, 2015).

SLOPE/W, which is based on limit equilibrium (LE) theories, is also one component in a complete suite of GeoStudio. It can model a variety of stability problems with different slip surface shapes, pore water pressure conditions, soil properties and loading conditions (Ng and Pang, 2000; Oh and Vanapalli, 2010).

2.2 The Eulerian-based FE Method

The Eulerian-based FE method available in Abaqus/Explicit FE software is used in the present study for numerical analysis. Note that typical FE programs developed in a Lagrangian framework cannot simulate very large deformation in a large-scale landslide because the significant mesh distortion around the failure plane causes numerical instabilities and non-convergences of the solutions (Griffiths and Lane, 1999). In the numerical technique used in the present study, the soil is modeled as a Eulerian material which can 'flow' through the fixed mesh without causing numerical issues related to mesh distortion. Further details of the mathematical formulations of the Eulerian-based FE approach and its applications to large-deformation quasi-static/dynamic problems (e.g. onshore and offshore landslides) are available in previous studies (Benson, 1992; Benson and Okazawa, 2004; Dey et al., 2015, 2016; Islam et al., 2018).

In the present study, the Eulerian-based FE code is used to simulate both the transient and steady-state seepage. Currently, built-in coupled pore pressure-stress elements are not available in the Eulerian-based FE code in Abaqus to model the seepage. Therefore, thermal–hydraulic analogy theory is implemented in this study, to model the seepage with thermally coupled Eulerian elements (EC3D8RT, eight-node thermally coupled linear brick elements with reduced integration and hourglass control) available in Abaqus. Based on the analogy theory (Section 2.3), the total water pressure and pore pressure can be successfully calculated from the temperature.

2.3 Thermal–hydraulic Analogy

Hamann et al. (2015) simulated pile jacking into a fully saturated soil under partially drained conditions using Abaqus CEL. They modelled the soil as a two-phase medium with the thermally coupled Eulerian elements by considering the fluid flow analogous to heat transfer. In other words, an analogy exists between the Darcy's law for fluid flow (Eq. (1)) and heat conduction in a medium (Eq. (2)), which are the governing equations for the Darcy's law and heat conduction, respectively.

$$\mathbf{q} = \frac{\kappa}{\mu_w}(-\nabla p_w) \tag{1}$$

$$\mathbf{f} = k(-\nabla\theta) \tag{2}$$

where $\mathbf{q}$ = Darcy flux or Darcy velocity in porous media; κ = intrinsic permeability; μ_w = dynamic viscosity; p_w = pore water pressure or total head pressure; $\mathbf{f}$ = heat flux; k = thermal conductivity; and θ = temperature. From Eqs. (1) and (2), it can be concluded that $p_w :: \theta$, $\mathbf{q} :: \mathbf{f}$, $\kappa/\mu_w :: k$ ("::" is a symbol of analogy). Therefore, the relationship between the thermal parameters and the seepage parameters can be developed as Eqs. (3–5) (Hamann et al., 2015).

$$k :: \frac{\kappa}{\mu_w} = \frac{K\mu_w/\gamma_w}{\mu_w} = \frac{K}{\gamma_w} \tag{3}$$

$$c :: \frac{1}{Q\rho} \tag{4}$$

$$\rho = (1-n)\rho_s + n\rho_w \tag{5}$$

where K = hydraulic conductivity; γ_w = specific weight (unit weight) of water; c = specific heat; Q = bulk modulus of the

mixture of fluid and soil particles; ρ = density of the soil; n = porosity of the soil; ρ_s = density of the solid grains; ρ_w = density of water.

To describe the behavior of the fluid phase in a porous media, a continuity equation (Eq. (6)) is applied by Lewis and Schrefler (1998):

$$div\left\{\frac{\kappa}{\mu_w}[-\nabla p_w - \rho_w(\mathbf{a}_{ws} + \mathbf{a}_s) + \rho_w \mathbf{b}]\right\} + \alpha_{biot}\mathbf{m}\dot{\boldsymbol{\varepsilon}}_s + \frac{\dot{p}_w}{Q} = 0 \quad (6)$$

where $\mathbf{a}_{ws}$ = relative acceleration of the fluid phase with respect to the soil skeleton; $\mathbf{a}_s$ = acceleration of the soil skeleton; $\mathbf{b}$ = body force per unit mass; $\mathbf{m}$ = second order unit tensor; $\dot{\boldsymbol{\varepsilon}}_s$ = strain rate of the solid skeleton. The first term of Eq. (6), meaning the diffusion of pore water, is solved by heat conduction within the temperature–displacement analysis procedure of Abaqus ($\mathbf{a}_{ws}$ is small and thus being neglected (Zienkiewicz et al., 1999); $\mathbf{a}_s$ remains zero when simulating the steady-state seepage); and the second term, meaning the change of pore pressure due to volumetric straining of the solid skeleton $\alpha_{biot}\mathbf{m}\dot{\boldsymbol{\varepsilon}}_s$, is not necessary to be calculated for the purpose of simulating initial steady-state seepage.

SEEP/W also neglected the change of pore pressure due to the volumetric strain of the solid skeleton. The governing differential equation used in SEEP/W finite element formulation is:

$$\frac{\partial}{\partial x}\left(K_x\frac{\partial H}{\partial x}\right) + \frac{\partial}{\partial y}\left(K_y\frac{\partial H}{\partial y}\right) + F = m_w\gamma_w\frac{\partial H}{\partial t} \quad (7)$$

where H = total head; K_x and K_y: hydraulic conductivity in the x and y directions, respectively; F = applied boundary flux (usually equals to 0); m_w = slope of the storage curve ($\partial\theta_v = m_w\partial p_w$, θ_v = volumetric water content, and p_w = pore water pressure or total head pressure); γ_w = the unit weight of water; and t = time. In the saturated region, m_w becomes equivalent to m_v, the coefficient of volume compressibility (Krahn, 2004). Equation (7) is the same equation of Eq. (6) ignoring the term $\alpha_{biot}\mathbf{m}\dot{\boldsymbol{\varepsilon}}_s$, and m_w is equivalent to $1/Q$. Therefore, the same results should be obtained when simulating the same seepage problem by using the Eulerian-based finite element model (with thermal-fluid analogy) and SEEP/W. Note that *K* and m_v in SEEP/W, and *k* and *c* in Abaqus influence only the transient state of analysis.

3 PROBLEM DEFINITION

An embankment consisted of sandy soil is studied. The geometry of the embankment is shown in Fig. 1. The embankment is 12 m high, 52 m base width, and an 8-m drainage is located at the toe of the downstream of the embankment. A rapid fill in the reservoir is considered. The water level of the reservoir is assumed to raise from 0 m to 11 m instantaneously (Fig. 1). Note that this assumption may not be able to reflect a realistic scenario. The transient seepage inside the embankment within 8 hours is studied using both the Eulerian-based FE method and SEEP/W. The results of the two methods are compared including the variation of the total water head distribution with time, the effective stresses distribution and factor of safety of the embankment. Furthermore, the progressive failure with strength reduction method is simulated using the Eulerian analysis.

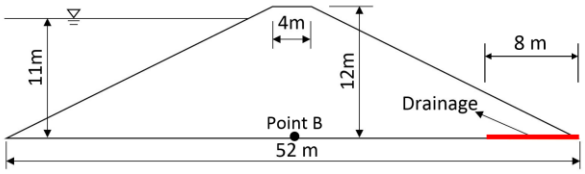

Figure 1. Geometry of rapid reservoir fill

4 FINITE ELEMENT MODELING

4.1 Load and Boundary Conditions

To simulate the rapid fill of the reservoir in SEEP/W analysis, a total head of 11 m is applied to the upstream surface of the embankment in an infinitely small time interval (blue line in Fig. 2(a)), and a total head of 0 m is applied to the drainage at the bottom of the embankment at downstream area (red line in Fig. 2(a)). On the other hand, adopting the fluid-thermal analogy, temperature boundary conditions are applied to the Eulerian model. A temperature boundary condition of 107910 °C (ρgh = 1000×9.81×11) is applied to the upstream of the embankment representing an 11 m total head (blue line in Fig. 2(b)), and a 0 °C boundary condition is applied to the area of the drainage (red line in Fig. 2(b)). The transient seepage analysis and transient thermal analysis for an 8-h time period are performed in SEEP/W and Abaqus CEL, respectively.

Based on the steady-state seepage results, the in-situ stresses are established in SIGMA/W and the Eulerian-based FE code, respectively. The gravity load is applied to the soils for both models. Zero displacement and zero velocity are implemented on the bottom of both SIGMA/W and the Eulerian-based FE code, respectively.

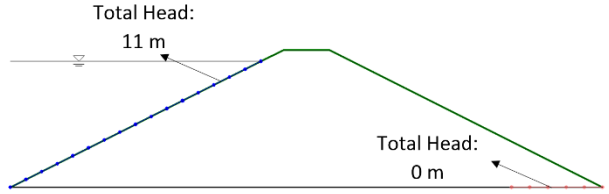

(a) SEEP/W model

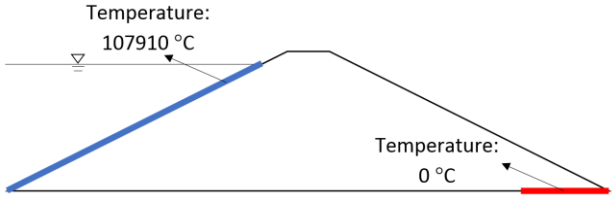

(b) Abaqus CEL model

Figure 2. Load and boundary conditions used for the embankment

The Eulerian-based FE code can model only three-dimensional condition. Therefore, the plane strain condition is simulated using the model thickness of one

element in the out of plane direction. A uniform mesh size (0.25 m x 0.25 m x 0.25 m) is used for all the Eulerian-based FE analyses.

4.2 Soil Parameters

The soil parameters used in the GeoStudio and Eulerian-based FE code are shown in Table 1. Medium dense sand is assumed as the filling material of the embankment. The soil is modeled using the Mohr-Coulomb model and the analyses are performed for the drained condition. The soil density, ρ is calculated from Eq. (5). The thermal parameters for the Eulerian analysis, i.e. thermal conductivity, k and specific heat, c, are calculated using Eqs. (3) and (4), respectively.

Table 1. Soil parameters used in numerical analyses

Young's modulus, E (MPa)	50
Poisson's ratio, ν	0.25
Porosity, n	0.35
$1/Q$ or m_v, (MPa^{-1})	0.02
Density of soil, ρ (kg/m^3)	2076
Hydraulic conductivity, K (m/s)	1×10^{-5}
Cohesion, c' (kPa)	1
Effective friction angle, φ′ (°) (Eulerian model)	40 to 28.5
Dilation angle, ψ (°) (Eulerian model)	15 to 0.625
Effective friction angle, φ′ (°) (SLOPE/W)	40 and 28.5

Note: The dilation angle ψ is calculated from $\varphi' - \varphi_c' = 0.8\psi$ (Bolton, 1986), where the φ_c' (the critical state friction angle) is assumed to be 28°.

5 FINITE ELEMENT RESULTS

5.1 Seepage Analysis

Both SEEP/W and the Eulerian-based FE models reached steady-state within 4 h, based on the total head distribution. The total head distributions inside of the embankment at 0.5 h and 4 h in SEEP/W are shown in Figs. 3(a) and 4(a), respectively. The temperature distributions at 0.5 h and 4 h in the Eulerian-based FE model are shown in Figs. 3(b) and 4(b), respectively. Note that, the temperature 9810 °C is equivalent to 1 m total head, based on the thermal–hydraulic analogy. To better compare the results of SEEP/W and the Eulerian-based FE model, the equivalent total head at point B (midpoint of the bottom of the embankment, as shown in Fig. 1) with time is plotted in Fig. 5. As can be observed in Figs. 3-5, the results from the Eulerian-based FE model perfectly matches the SEEP/W results. The comparison strongly supports the effectiveness of the thermal–hydraulic analogy in the present Eulerian-based FE model. Also, the relationships between thermal and seepage parameters (Eqs. (3–5)) are validated.

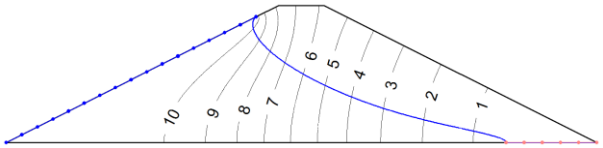

a) Total head at t = 0.5 h in SEEP/W (unit: m)

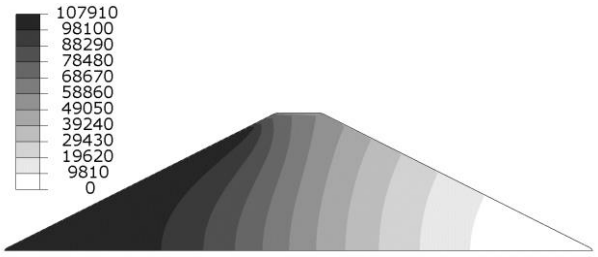

b) Temperature distribution or total head pressure at t = 0.5 h in Eulerian-based FE model (unit: °C or Pa)

Figure 3. (Equivalent) Total head distribution after 0.5 h

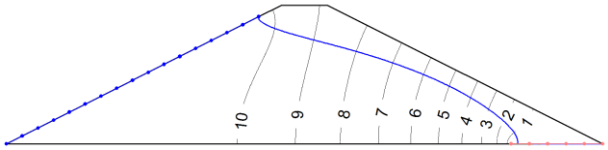

(a) Total head at t = 4 h in SEEP/W (unit: m)

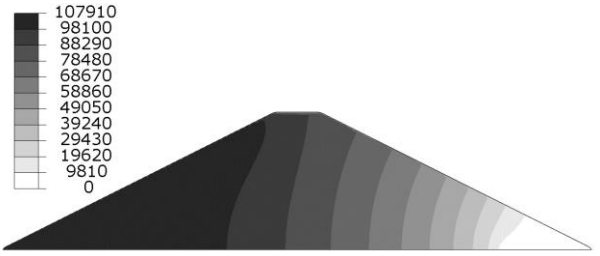

(b) Temperature distribution or total head pressure at t = 4 h in Eulerian-based FE model (unit: °C or Pa)

Figure 4. (Equivalent) Total head distribution in the embankment at 4 h

Fig. 5 shows that the total head becomes a constant after t ~ 4 h. At the same time, not only point B reaches a constant total head, but also other parts of the embankment come to the steady state. For the in-situ situation, the seepage condition usually remains steady-state when the boundary conditions do not change significantly in a short period. Therefore, only the steady-state seepage is considered for in-situ stresses modeling.

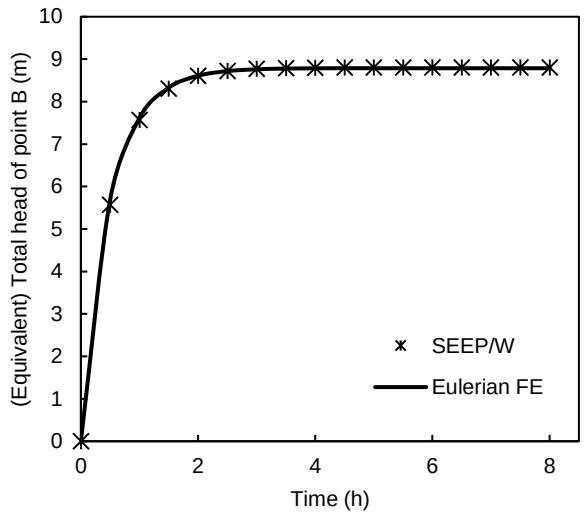

Figure 5. (Equivalent) Total head at point B

5.2 In-situ Stresses

The distribution of in-situ stresses can directly influence the location of the critical slip surface. Therefore, it is important to accurately establish the in-situ stresses, in order to effectively analyze slope stability.

Based on the results of the equivalent total head, the seepage forces can be calculated and then applied to the Eulerian elements under the phreatic line. Coupled with the gravity load, the in-situ stresses under the seepage condition are modeled using the Eulerian-based FE code. The vertical, horizontal, and deviatoric (von Mises) stresses obtained from the Eulerian-based FE modeling are presented in Figs. 6(a), 7(a) and 8(a), respectively. For comparison, the in-situ stresses calculated from SIGMA/W, together with seepage analysis results from SEEP/W, are shown in Figs. 6(b), 7(b) and 8(b).

From the comparison, the in-situ stress distributions are found to be quite similar between the Eulerian-based FE and SIGMA/W analyses. The maximum vertical stresses in SIGMA/W and the Eulerian-based FE code are 136.2 kPa and 137.1 kPa, respectively (Fig. 6). Furthermore, SIGMA/W and the Eulerian-based FE code calculate the maximum horizontal stress of 48.2 kPa and 44.9 kPa, respectively (Fig. 7). For the maximum deviatoric stress, the values are 97.6 kPa and 100.5 kPa in SIGMA/W and the Eulerian-based FE, respectively (Fig. 8). This slight difference is potentially due to the solution algorithms used in these software packages.

5.3 Slope Stability and Deformation Analysis

In the present study, the strength reduction method is used to trigger the failure of the slope and find the slip surface from the Eulerian-based FE analysis. To conduct the strength reduction, the effective friction angle (φ') is decreased from 40° to 28.5°. The dilation angle (ψ) is also reduced accordingly as $\psi = (\varphi' - \varphi_c')/0.8$ (Bolton, 1986). Furthermore, the slope stability analysis is conducted with the limit equilibrium method using SLOPE/W, based on the in-situ stresses from SEEP/W (considering seepage result). The Spencer method is selected for the calculation of factor of safety and slip surfaces in SLOPE/W.

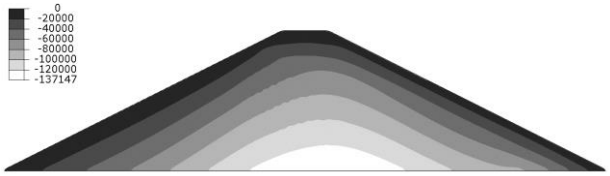

a) Eulerian-based FE (unit: Pa)

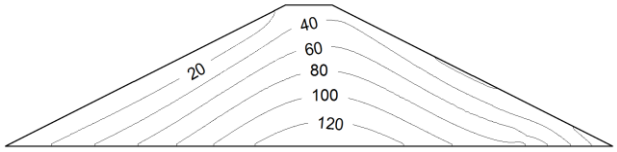

b) SIGMA/W (unit: kPa)

Figure 6. Vertical stress under steady-state seepage

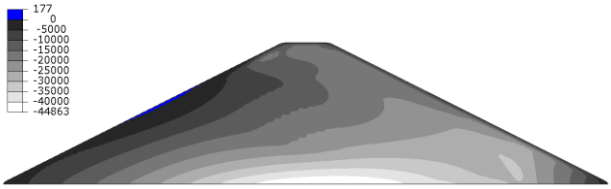

a) Eulerian-based FE (unit: Pa)

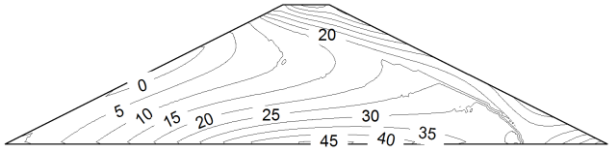

b) SIGMA/W (unit: kPa)

Figure 7. Horizontal stress under steady-state seepage

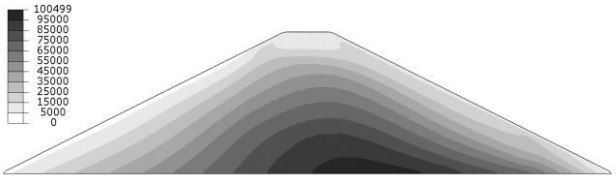

a) The Eulerian-based FE code (unit: Pa)

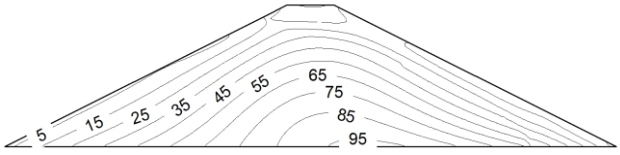

b) SIGMA/W (unit: kPa)

Figure 8. Deviatoric stress under steady-state seepage

The accumulated plastic shear strain in the Eulerian FE analysis for different friction angles (φ' = 40°, 30° and

28.5°) is shown in Figs. 9(a), 9(b) and 9(d), respectively. The slope is stable, and no plastic shear strain develops in the soil elements for φ′ = 40° (Fig. 9(a)). The failure plane does not form instantaneously rather the failure starts from the toe of the slope and gradually progresses to the left and up (Fig. 9(b)). As shown in Fig. 9(d), a complete failure plane forms when the shear strength is reduced significantly (e.g., φ′ = 28.5°). Figure 9(c) shows the instantaneous velocity vector of the soil elements above the failure plane.

For comparison, the critical slip circles and factor of safety for these values of φ′ obtained from SLOPE/W analysis are also shown in Fig. 9. The slight difference between the location of the critical circle in SLOPE/W and high shear strain zone in FE analysis is potentially due to the progressive formation of the failure plane and displacement of the failed soil mass in the latter one. The FOS ~ 1.0 for φ′ = 28.5° (Fig. 9(d)).

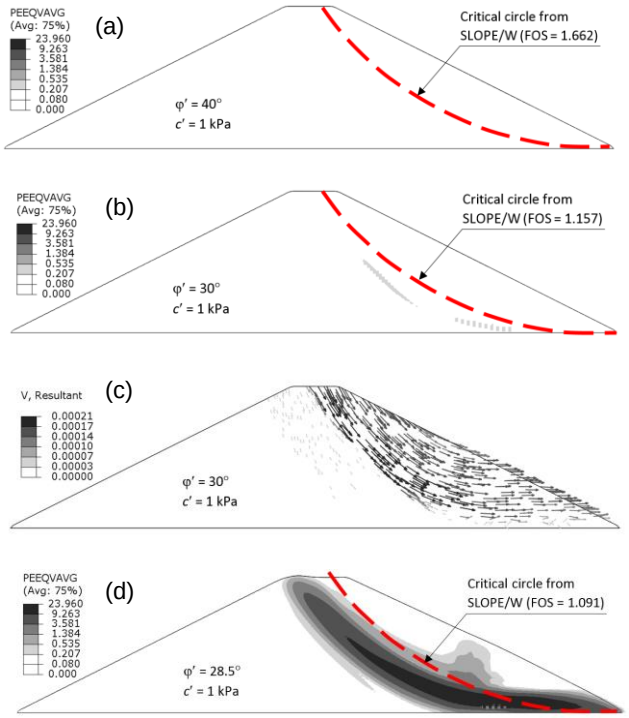

Figure 9. Plastic shear strain and instantaneous velocity vectors in slope stability analysis

5.4 Influence of Seepage Forces on Slope Failure

If the seepage force is not considered in the model, the failure pattern is usually different. To demonstrate it, the same problem as presented in Section 5.3 is analyzed using the Eulerian FE approach. In this case, the seepage force is not added to the soil elements; however, the buoyancy is still applied to the soil elements below the phreatic line. Figure 10 shows that the in-situ deviatoric stress is very different from the values obtained with seepage effects (compare Figs. 8(a) and 10).

Using the same strength reduction approach presented in Section 5.3, the stability of the slope is checked without considering the seepage. The slope remains stable in this case (i.e., without seepage) even for φ′ = 28.5° while it fails when the seepage force is considered (Fig. 9(d)). In other words, seepage force significantly influences the result of slope stability analysis because of the change in in-situ effective stresses.

In a large-scale landslide modeling, the in-situ seepage conditions might be important, especially in triggering of the landslide by the failure of the first soil block.

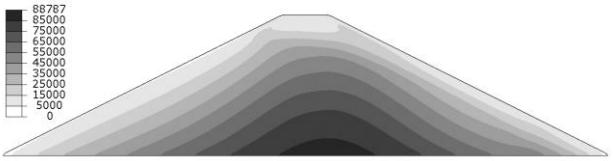

Figure 10. Deviatoric stress in Eulerian-based FE analysis without seepage forces (unit: Pa)

6 CONCLUSIONS

In this study, a technique is developed to model the seepage for finite element modeling of slope failures using the Eulerian-based FE code. Both transient and steady-state seepage conditions are modeled based on the thermal–hydraulic analogy. The FE results are comparable to those obtained from SEEP/W analysis. The in-situ stresses at the steady-state seepage condition are modeled in both the Eulerian-based FE model and SIGMA/W. The two methods give nearly identical results. Furthermore, the location of the critical failure plane inferred from the Eulerian-based FE analysis and obtained from SLOPE/W is similar. However, the SLOPE/W could not handle the post-failure process while the Eulerian-based FE model can simulate the complete failure mechanisms.

In conclusion, the technique developed in the present study is applicable to slope stability analysis considering the seepage effects in the Eulerian-based FE code. Coupled with its advantage to handle large deformation analysis, the progressive landslides, e.g. the 2010 St. Jude Landslide, can be modeled with the consideration of both seepage effects and large deformation. Note that the simulation results presented in this study is only for idealized soil properties and boundary conditions; however, the developed technique could be used case specific scenarios.

ACKNOWLEDGEMENTS

The works presented in this paper have been supported by the Natural Sciences and Engineering Research Council of Canada (NSERC), InnovateNL and former Research and Development Corporation of Newfoundland and Labrador (RDC).

REFERENCES

Benson, D. J. 1992. Computational methods in Lagrangian and Eulerian hydrocodes. *Computer methods in Applied Mechanics and Engineering*, 99 (2-3), 235–394.

Benson, D. J., and Okazawa, S. 2004. Contact in a multi-material Eulerian finite element formulation. *Computer methods in applied mechanics and engineering*, 193(39-41), 4277–4298.

Bolton, M. D. 1986. Strength and dilatancy of sands. *Géotechnique*, 36(1), 65–78.

Dey, R., Hawlader, B., Phillips, R. and Soga, K. 2015. Large deformation finite element modeling of progressive failure leading to spread in sensitive clay slopes. *Géotechnique*, 65 (8), 657–668.

Dey, R., Hawlader, B., Phillips, R. and Soga, K. 2016. Numerical modelling of submarine landslides with sensitive clay layers, *Géotechnique*, 66 (6), 454–468.

GeoStudio 2007. GEOSLOPE International Ltd. Calgary, AB, Canada.

Griffiths, D. V., and Lane, P. A. 1999. Slope stability analysis by finite elements. *Géotechnique*, 49 (3), 387–403.

Hamann, T., Qiu, G., and Grabe, J. 2015. Application of a Coupled Eulerian–Lagrangian approach on pile installation problems under partially drained conditions. *Computers and Geotechnics*, 63, 279–290.

Islam, N., Hawlader, B. C., Wang, C., and Soga, K. 2018. Large deformation finite-element modelling of earthquake-induced landslides considering strain-softening behaviour of sensitive clay. *Canadian Geotechnical Journal*, https://doi.org/10.1139/cgj-2018-0250.

Krahn, J. 2004. *Seepage modeling with SEEP/W: An engineering methodology.* GEO-SLOPE International Ltd. Calgary, Alberta, Canada.

Lane, P. A., and Griffiths, D. V. 2000. Assessment of stability of slopes under drawdown conditions. *Journal of Geotechnical and Geoenvironmental Engineering*, 126 (5), 443–450.

Lewis, R. W., and Schrefler, B. A. 1998. *The finite element method in the static and dynamic deformation and consolidation of porous media*. John Wiley, New York.

Locat, P., Fournier, T., Robitaille, D. and Locat, A. 2011. Glissement de terrain du 10 mai 2010, Saint-Jude, Montérégie – Rapport sur les caractéristiques et les causes. Ministère des Transports du Québec, Service Géotechnique et Géologie, Rapport MT11-01.

Ng, C. W., and Pang, Y. W. 2000. Influence of stress state on soil-water characteristics and slope stability. *Journal of Geotechnical and Geoenvironmental Engineering*, 126(2), 157–166.

Oh, W. T., and Vanapalli, S. K. 2010. Influence of rain infiltration on the stability of compacted soil slopes. *Computers and Geotechnics*, 37(5), 649-657.

Oh, W. T., and Vanapalli, S. K. 2011. Modelling the applied vertical stress and settlement relationship of shallow foundations in saturated and unsaturated sands. *Canadian Geotechnical Journal*, 48(3), 425–438.

Qi, S., and Vanapalli, S. K. 2015. Hydro-mechanical coupling effect on surficial layer stability of unsaturated expansive soil slopes. *Computers and Geotechnics*, 70, 68–82.

Saha, B., Hawlader, B., Dey, R., and McAffee, R. 2014. Slope stability analysis using a large deformation finite element modeling technique. In 67th Canadian Geotechnical Conference GeoRegina. Regina, Saskatchewan, Canada.

Zienkiewicz, O. C., Chan, A. H. C., Pastor, M., Schrefler, B. A., and Shiomi, T. 1999. *Computational geomechanics with special reference to earthquake engineering*, Wiley, New York.